ACS APPLIED MATERIALS & INTERFACES

www.acsami.org

Research Article

Effect of Poly(vinyl butyral) Comonomer Sequence on Adhesion to Amorphous Silica: A Coarse-Grained Molecular Dynamics Study

Christopher C. Walker, Jan Genzer, and Erik E. Santiso*

Cite This: *ACS Appl. Mater. Interfaces* 2020, 12, 47879–47890

Read Online

ACCESS | Metrics & More | Article Recommendations | Supporting Information

Downloaded via NORTH CAROLINA STATE UNIV on September 30, 2021 at 21:13:07 (UTC).
See https://pubs.acs.org/sharingguidelines for options on how to legitimately share published articles.

ABSTRACT: Modulating a comonomer sequence, in addition to the overall chemical composition, is the key to unlocking the true potential of many existing commercial copolymers. We employ coarse-grained molecular dynamics (MD) simulations to study the behavior of random-blocky poly(vinyl butyral-*co*-vinyl alcohol) (PVB) melts in contact with an amorphous silica surface, representing the interface found in laminated safety glass. Our two-pronged coarse-graining approach utilizes both macroscopic thermophysical data and all-atom MD simulation data. Polymer−polymer nonbonded interactions are described by the fused-sphere SAFT-γ Mie equation of state, while bonded interactions are derived using Boltzmann inversion to match the bond and angle distributions from all-atom PVB chains. Spatially dependent polymer−surface interactions are mapped from a hydroxylated all-atom amorphous silica slab model and all-atom monomers to an external potential acting on the coarse-grained sites. We discovered an unexpected complex relationship between the blockiness parameter and the adhesion energy. The adhesion strength between PVB copolymers with intermediate VA content and silica was found to be maximal for random-blocky copolymers with a moderately high degree of blockiness rather than for diblock copolymers. We attribute this to two main factors: (1) changes in morphology, which dramatically alter the number of VA beads interacting with the surface and (2) a non-negligible contribution of vinyl butyral (VB) monomers to adhesion energy because of their preference to adsorb to zones with low hydroxyl density on the silica surface.

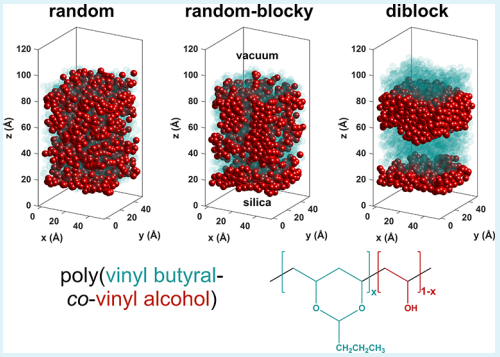

KEYWORDS: *polymer adsorption, silica, copolymer sequences, coarse-graining, molecular dynamics*

1. INTRODUCTION

Poly(vinyl butyral-*co*-vinyl alcohol) (PVB) is widely used in the automotive industry and in architectural applications as the principal component of the interlayer in laminated safety glass.[1] Typical laminated safety glass is composed of one or more layers of a polymer interlayer, roughly 0.5 mm in thickness, and glass panels, approximately 2 mm in thickness.[2] PVB is valued for its ability to impart toughness to glass/PVB/glass panels. Upon an impact on the composite material, the adhesion of PVB to glass in combination with the ability of PVB to dissipate energy prevents shattering of the glass into shards, which may cause harm.[3,4] Impact-resistant glasses are vital not only for vehicle safety but also for security applications and providing resistance to wind-borne debris during hurricanes and other severe storms.[5−7] Despite the widespread use of PVB-laminated safety glasses since the 1930s, the adhesion of PVB to glass remains poorly understand at the molecular level, hindering advancements in fundamental physical properties, such as toughness. With one monomer (VA) providing strong interaction with silanol moieties on the glass surface via hydrogen-bonding and the other (VB) providing energy dissipation properties, PVB copolymer presents an intriguing case for studying sequence−property relationships.

The chemical structure of the PVB copolymer is shown in Figure 1. PVB is synthesized by postpolymerization modification of poly(vinyl alcohol). Intramolecular acetalization of the glycol groups along the PVA chain occurs upon the addition of butyraldehyde in the presence of an acid catalyst, such as HCl. The overwhelming majority of acetal rings formed are six-membered dioxanes as most of the glycol groups in PVA are spaced on alternating carbons. Some 1−2 glycol sequences may be present in PVA,[7] which is most commonly synthesized by transesterification of poly(vinyl acetate). Still, these have been found to have a negligible effect on physical properties of PVA and are ignored for this study. PVB typically contains 1−2% by weight of residual acetate groups from impurities in the parent PVA chains;[7] these are also neglected here for simplicity. It is standard practice to add plasticizers or adhesion promoters to augment chain mobility or the strength of adhesion between

Received: June 12, 2020
Accepted: September 14, 2020
Published: September 14, 2020

ACS Publications

© 2020 American Chemical Society

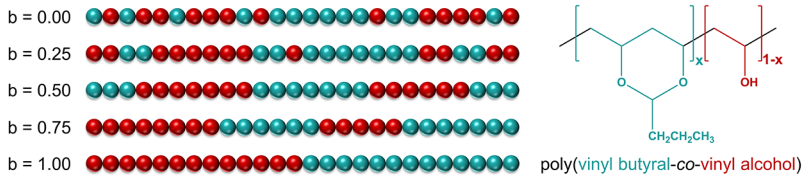

Figure 1. Monomer chemical structures of PVB and examples of comonomer sequences resulting from different blockiness parameters, with 50 mol % of each monomer type.

PVB and glass, respectively. For simplicity, we will consider only unmodified PVB copolymers in this work.

Copolymers can generally exhibit a diverse range of chemical and physical properties depending on the overall chemical composition and the sequence in which comonomers are spatially arranged in the chain. Much of this astronomically ample design space is, however, unexplored with the vast majority of previous studies focusing on "perfectly random," alternating, or diblock copolymers. Few have investigated structure−property relationships in synthetic copolymers with sequences of various blocks that are randomly distributed or arranged in irregular patterns. Advances in synthetic polymer chemistry allowing for improved control over copolymer sequences and architectures,[8−11] in combination with molecular simulations and machine-learning techniques, are giving rise to a new field of polymer sequence engineering in which it is becoming possible to design sequences which optimize target physical properties.[12−24] Exercising control over copolymer sequences has the potential to significantly improve the performance of the existing commercial copolymers.

Theoretical and simulation studies have played a key role in understanding the effect of monomer sequence and chain architecture on copolymer phase behavior and interfacial phenomena. Whereas precise control over the polymer sequence is tedious and limited to low-molecular weight chains or multiblock architectures in experiments, it is trivial in simulation methods such as molecular dynamics. Simulation approaches also allow for direct observation of nanoscopic detail at interfaces. However, studying polymer phenomena such as adsorption of a polymer melt, which occurs over long times and large length scales, at the atomistic resolution, remains a formidable challenge. The development of accurate and transferable coarse-grained polymer force fields, which aim to capture macroscopic thermophysical properties, structural properties of high-resolution atomistic models, or ideally both, remains a highly active field of research. Numerous reviews have chronicled the development of such "systematic" coarse-graining techniques for polymers.[25−28] Apart from particle-based simulations of polymers, other theoretical methods including self-consistent field theory (SCFT)[29−32] and integral-equation approaches such as polymer reference interaction site models (PRISM)[33,34] have been used extensively to study copolymer morphology and interfacial behavior.

Previous simulation studies have mainly concentrated on polymer adsorption to flat or crystalline surfaces.[21,35−43] However, surface roughness and chemical heterogeneity are expected to play critical roles in determining interfacial properties. Studies that have compared polymer adsorption onto different surfaces have demonstrated marked differences in the polymer−solid interfacial structure, such as the local polymer density at the interface and orientation of vinyl functional groups.[44] The cartoon in Figure 2, depicting copolymer adsorption onto a flat surface, thus represents a

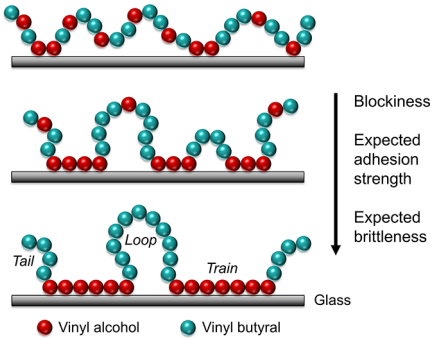

Figure 2. Expected influence of PVB blockiness on adhesion strength and interfacial toughness.

rather primitive view of copolymer adsorption in this regard. In this work, we investigate the interfacial structure and adhesion properties of random-blocky copolymers at a heterogeneous rough surface. This comprehensive study of the effects of both blockiness and composition on copolymer melt adhesion to amorphous silica is, to our knowledge, the first of its kind.

Polymer adhesion to a solid substrate is fundamentally different than the case of small molecules, in that the adsorption of a functional group on one monomer to a substrate influences the chain conformation and thus the adsorption of other monomers. Clearly, a diblock copolymer and a random copolymer will give rise to different adhesion properties (Figure 2). Blocks of VA monomers will segregate toward the surface and provide strong adhesion, but the low mobility of the adsorbed VA blocks will lead to a highly brittle PVB/glass composite. In contrast, a random PVB copolymer is expected to have a lower number of VA−silanol contact points, leading to lower adhesion but higher mobility in the vicinity of the interface. Similar arguments may be made in terms of overall chemical composition of PVB: if a PVB copolymer with a high VA content is used, adhesion strength will be high, but the glass/PVB composite material will be brittle as the strongly adsorbed chains are conformationally trapped. If the PVB contains too little VA content, the adhesion will be too weak to contain the fracturing glass shards upon impact. Of interest in this work is the combined effects of vinyl alcohol content and the degree of blockiness, the length of consecutive runs of the same monomer type, on the adhesion strength of PVB. While it is already well-established that adhesion strength of random PVB copolymers to glass increases with VA content,[45] we hypothesize that manipulation of the sequence distribution of VA and VB monomers could provide control over both adhesion strength and local chain stiffness at the interface, allowing for optimization of the fracture toughness of glass/PVB/glass composite materials. As will be seen, the situation for copolymer adsorption onto heterogeneous surfaces is more complex than Figure 2 suggests. Figure 1 shows a representative sampling of sequences with different degrees of blockiness (b), ranging from

https://dx.doi.org/10.1021/acsami.0c10747
ACS Appl. Mater. Interfaces 2020, 12, 47879−47890

"truly random" ($b = 0.00$) to diblock ($b = 1.00$). The procedure used to generate sequences with a given blockiness is described in Section 2.3.

In this work, we use coarse-grained molecular dynamics (MD) simulations to study the PVB−glass interface, varying the overall chemical composition and sequence distributions of PVB copolymers. Faster dynamics, a large reduction in the number of particles, and a simpler interaction potential dramatically improve the computational efficiency compared to all-atom MD simulation. Our approach, outlined in the following section, combines the fused-sphere SAFT-γ Mie group-contribution equation of state (EoS),[46] structural data from all-atom MD simulations of polymer chains, and forces mapped from a realistic all-atom amorphous silica model.

2. SIMULATION METHODOLOGY

2.1. Fused-Sphere SAFT-γ Mie Force Field. In a previous study,[47] we developed a coarse-grained force field for PVB copolymers using the fused-sphere SAFT-γ Mie EoS.[46] VA monomers are represented by a single spherical bead and VB monomers are represented by four spherical beads arranged in a geometry which preserves both the ring character and a distinct hydrophobic tail (Figure 3). Our hybrid top-down/bottom-up coarse-graining strategy introduced in ref 48 and extended to PVB copolymers in ref 47 uses experimental vapor−liquid equilibria data to fit nonbonded parameters and bond and angle potentials derived to reproduce the corresponding atomistic structural distribution. The inclusion of appropriate chain stiffness is critical for the study of the PVB interfacial system. Several studies have found that the conventional fully flexible tangent-sphere SAFT-γ Mie chains do not accurately reproduce properties such as surface and interfacial tension, but that this issue can be largely overcome by the addition of bond angle-bending potentials.[49−53] Whereas these studies added angle potentials independent of the SAFT-γ Mie EoS to tangent-sphere chains, our fused-sphere approach incorporates bond and angle potentials into the nonbonded parameter optimization. From coarse-grained NPT MD simulations in which the bond and angle potentials derived from a higher-resolution reference system are used, the bead overlap parameter and its associated optimal Mie parameters are determined by matching with the polymer or oligomer density. This target density can be taken from a literature database or computed using the fine-grained reference force field.

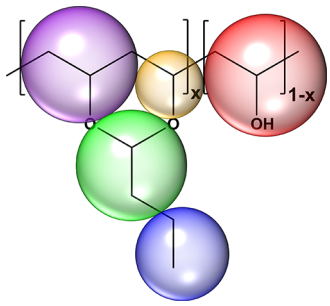

Figure 3. Coarse-grained SAFT-γ Mie model for PVB copolymers. The parent molecules of each bead and mapping function are given in ref 47. The coarse-grained beads are bonded at all points of co-tangency shown, and angle potentials are used for all possible angles except those involving the side chain alkyl bead shown in dark blue, which retains nonbonded interactions with 1−3 neighbors instead. For clarity, the bead overlap is not depicted here.

Optimal Mie parameters and the shape factor for PVA were taken from the original homopolymer fused-sphere SAFT-γ Mie model.[48] With the PVA parameters fixed and standard SAFT-γ Mie mixing rules applied,[46] the parameters for the vinyl butyral beads were optimized to reproduce the density of a random PVB copolymer with 50 mol % VA monomers. As the square-well association site scheme[46] was not used to model directional hydrogen-bonding interactions explicitly, a PVB model fit only to PVB homopolymer density did not provide an accurate representation of copolymer density as a function of VA content. VA−VB interactions were overestimated in that case as hydrogen bonding interactions were effectively included in the PVA standard Mie parameters. A model fit to the density of a 50 mol % VA copolymer provided a much-improved representation of PVB−PVA cross-interactions, resulting in excellent agreement with the all-atom PVB copolymer density for all but the case of very low (i.e., less than ∼10 mol %) VA content. Glass-transition NPT MD simulations using the fused-sphere SAFT-γ Mie PVB copolymer model resulted in calculated T_g, in agreement with experimental values for compositions ranging from 12 to 75 mol % VA content. Further details on the PVB SAFT-γ Mie force field, including the Mie parameters, shape factors, and bonded potentials, may be found in ref 47.

2.2. Force-Mapping Silica−PVB Interactions. The SAFT-γ Mie EoS on its own cannot directly model interfacial systems, so surface−polymer interactions must be derived from an additional model. SAFT equations of state have been coupled with classical density functional theory (DFT) to enable the study of interfaces and polymer morphology without the need for MD simulation.[54−56] However, because of the way that shape factors are used as an effective parameter of polymer chains in the fused-sphere SAFT-γ Mie polymer force field,[47,48] the Helmholtz energy of the polymers is not directly calculable from the SAFT-γ Mie EoS. Moreover, shape factors are not well-defined in the SAFT + DFT framework.[54] To capture surface roughness and spatial heterogeneity of silanol moieties on the silica surface, which are critical factors in influencing adhesion properties, we chose to map the interaction forces between a realistic all-atom amorphous silica slab model and all-atom VB and VA monomers.

We employed an all-atom amorphous silica slab model developed by Black et al.[57] using the ReaxFF force field[58] and surface-functionalized with silanols following the procedure outlined in ref 57. Silanol surface density matches the experimental literature value[59] of ∼5 nm^{-2}. Visualizations of the slab model, which is 50 Å × 50 Å in area and ∼20 Å in thickness, are shown in Figure 4.

The all-atom optimized potentials for liquid simulations (OPLS-AA) force field[60] was used to represent the VB and VA monomers, and OPLS-AA parameters modified for silica[61] were used for the slab model. The all-atom force field parameters for PVB are provided in the Supporting Information of ref 47. To obtain configurationally averaged forces between the slab and VB and VA monomers, short MD simulations of all-atom monomers with OPLS-AA parameters were run with the corresponding coarse-grained particle centers-of-mass fixed to each coordinate over a 3-dimensional (3D) grid. The large-scale atomic/molecular massively parallel simulator (LAMMPS) software package[62] was used for all MD simulations in this work. The forces exerted by the silica slab on each bead type as a function of x, y, and z coordinates of the bead centers were fit to a

https://dx.doi.org/10.1021/acsami.0c10747
ACS Appl. Mater. Interfaces 2020, 12, 47879−47890

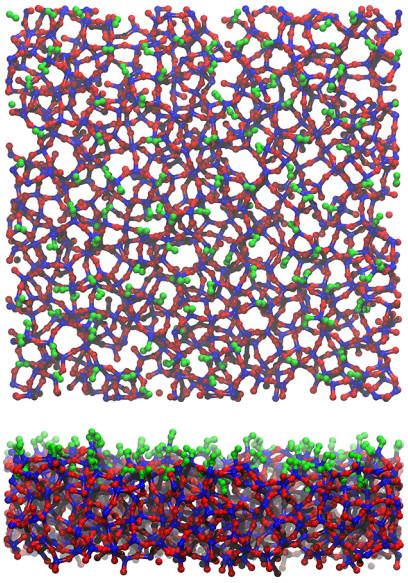

Figure 4. Top-down (top) and cross-sectional (bottom) view of all-atom amorphous silica slab functionalized with silanols. Silicon atoms are represented by blue spheres, internal oxygens by red spheres, and hydroxyls by green spheres.

3D spline function and implemented as an external potential in the coarse-grained PVB−silica MD simulations. Further details regarding the force-mapping procedure and its implementation are outlined in the Supporting Information.

2.3. Coarse-Grained PVB Adsorption MD Simulation. To generate copolymer sequences with tunable distributions in blockiness, we devised a simple algorithm with a single blockiness parameter, b, which varies from 0, representing a "truly random" copolymer with an uncorrelated sequence, to 1, representing a diblock copolymer. First, a pool of monomers is created based on the target molecular weight and the overall chemical composition of the copolymer. The first monomer is randomly selected from the pool. For each subsequent monomer, a random number r between 0 and 1 is generated. If $r \leq b$, the next monomer in the sequence is the same as the previous unless that monomer type is depleted from the pool. If $r > b$, the following monomer in the sequence is randomly selected from the pool. The result is a Poisson-like distribution in block length.

To study the effect of overall composition and blockiness on adhesion strength, we systematically varied the blockiness and overall chemical composition in interfacial MD simulations. Each system contained 50 chains of ∼2.4 kDa molecular weight with independently generated sequences. To maintain this molecular weight, the numbers of VA and VB monomers (N_{VA} and N_{VB}) were varied, as shown in Table 1. For each blockiness and chemical composition, we ran three simulations with independent sequence distributions. The mean block lengths of VA type and VB type for each case are shown in Figure 5, and a visual representation of how the blockiness parameter affects the VA and VB block sequences is shown in Figure 1. Illustrative sequences were chosen by random selection of one of the 50 chains for a given blockiness. At first glance, even the "truly random" 50 mol % VA copolymer appears to be surprisingly blocky. Its defining feature, however, is a high number of isolated monomers (blocks of length 1). The $b = 0.25$ chain has the most doublet blocks, while blocks with 1 or 2 monomers are increasingly rare at $b = 0.50$ and above.

Table 1. Chemical Compositions of the PVB Chains

mol % VA	wt % VA	vol % VA[a]	N_{VA}	N_{VB}
0	0	0	0	17
25	9.36	8.45	5	15
50	23.7	21.7	13	13
75	48.2	45.4	27	9
100	100	100	54	0

[a]Volume percent is computed from approximating bead volume as $(\pi/6)r_o^3S$, in which S is the shape factor in the fused-sphere SAFT-γ Mie model and r_o is the equilibrium self-interaction distance defined in the Mie potential.

In adhesion simulations, chains were first packed[63] into an elongated simulation cell with dimensions of 50 Å × 50 Å × 370 Å and migrated toward the interfacial region over a short NVT simulation by adding an artificial force in the z-direction. The simulation box was then cropped in the z-dimension to 150 Å. The system was annealed at 1000 K for 20 ns to remove dependence on the initial configuration. Further simulated annealing was then performed for 20 ns each at 800, 700, and 600 K, and for 40 ns at 500 K with cooling intervals defined by a rate of 20 K/ns. An artificial biasing force of −0.05 kcal/mol/Å was added to all beads at each 1 fs time step to promote adsorption and removed after cooling to 500 K. After the annealing period at 500 K, each copolymer system was cooled to 400 K and equilibrated for 150 ns. Convergence of the simulations was determined by block averaging of the PVB−silica interaction energy and the total system energy, along with inspection of the 3D morphology at 10 ns intervals. Figure S32 in the Supporting Information shows the PVB−silica interaction energy as a function of equilibration time at 400 K, averaged over 10 ns blocks. The relative strengths of PVB−silica interaction energy as a function of VA content and blockiness are maintained throughout the entire 150 ns equilibration period, confirming the effectiveness of the rigorous simulated annealing procedure employed here.

3. RESULTS AND DISCUSSION

It is first useful to review the overall morphologies that resulted from the MD simulations of each of the 15 different copolymers studied (Figure 6). In these 3D representations, the PVB−silica interface is located at low z and the PVB−vacuum interface is located at high z. Beads are represented by their Mie volumes, as discussed in the Table 1 footnote. It is clear that for each of the three different overall VA monomer fractions, with increasing blockiness, phase segregation away from the interface becomes more pronounced. For diblocks, lamellae of alternating VA and VB blocks form for only the case of approximately equal volume fractions of VA and VB monomers (75 mol %), as expected. For the 50 mol % VA diblock, a cylindrical domain of VA monomers forms below a thin layer of VB monomers near the top of the melt. For the lowest VA monomer fraction (25 mol % or 8.45 vol % VA), small spherical domains of VA are observed. In all cases, VB is highly enriched at the vacuum interface, as expected, because of its substantially lower surface energy compared to the VA beads, which have a stronger self-interaction. For 50 and 75 mol % VA systems of intermediate blockiness ($b = 0.25$ to $b = 0.75$), the morphology is more complex and warrants further analysis. In particular, $b = 0.75$ and 75 mol % VA resembles partially formed lamellae.

Several trends are also apparent at the PVB−silica interface. At 25 mol % VA content, there is not enough VA present near

https://dx.doi.org/10.1021/acsami.0c10747
ACS Appl. Mater. Interfaces 2020, 12, 47879−47890

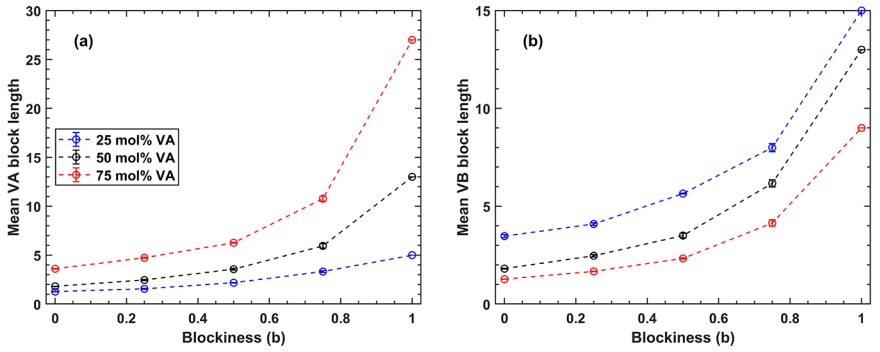

Figure 5. Mean VA (a) and VB (b) block lengths for 25 mol % VA (blue), 50 mol % VA (black), and 75 mol % VA (red) copolymer chains with a fixed molecular weight of ∼2.4 kDa. Error bars represent the standard error of the mean of the three independent trials.

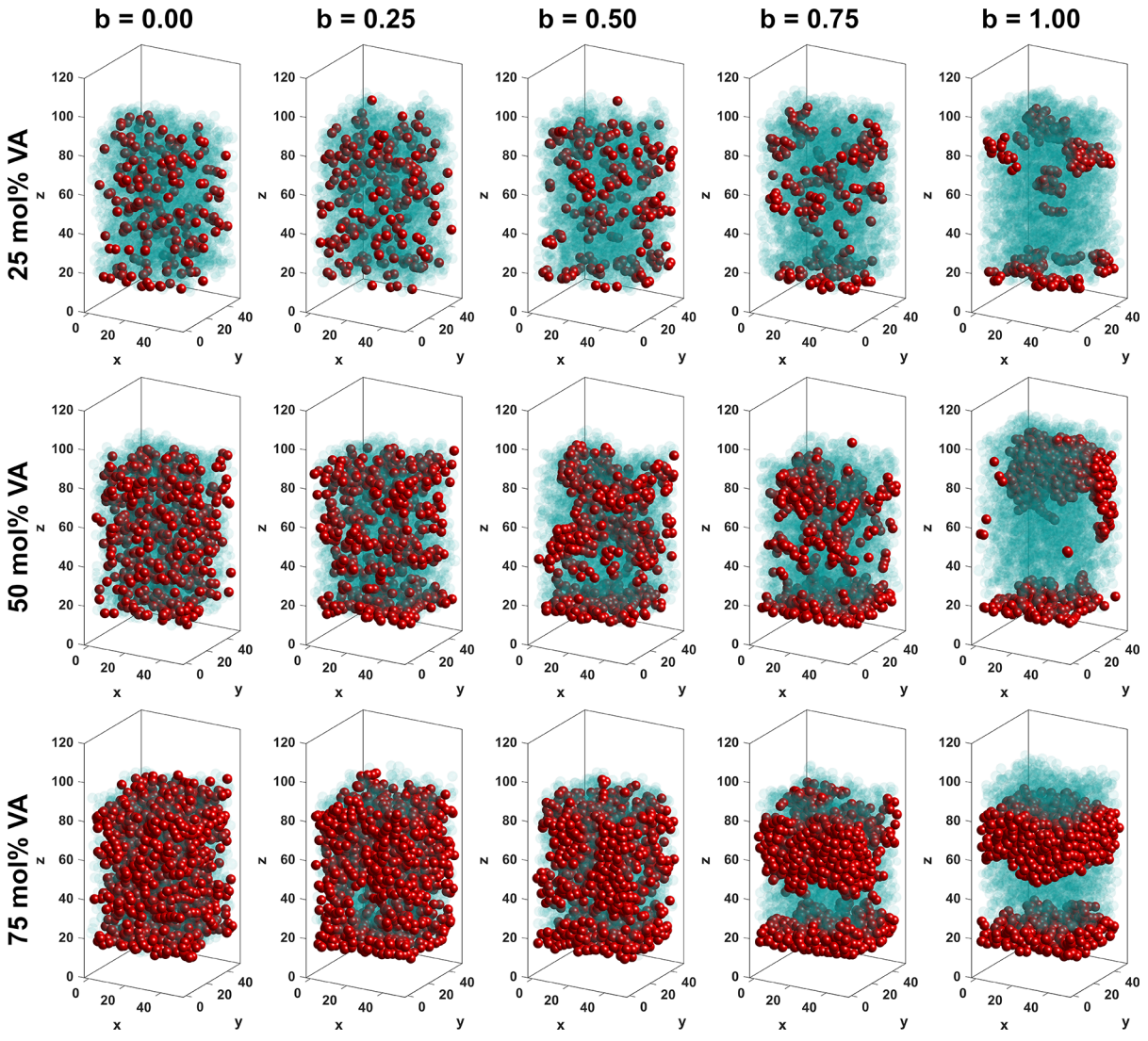

Figure 6. Visualization of 3D morphology for PVB copolymers at the interface with silica (located at the lower region at approximately z = 20 Å), as a function of VA content and blockiness parameter used to generate the comonomer sequences. One of the three independent trials is shown as a representative example of each VA content and blockiness. Red beads represent VA monomers and semi-transparent cyan beads represent VB monomers. All beads are depicted as spheres with diameters equal to their equilibrium Mie self-interaction distance, scaled by their shape factors, and all simulation snapshots are taken after 150 ns of equilibration at 400 K.

the interface to allow for full coverage by VA monomers, even for the diblock case. For 50 mol % VA content, manipulation of blockiness allows for a wide breadth of VA contact fractions to be achieved (Figures 7 and 9). The diblock system features nearly exclusively VA monomers contacting with the surface (∼94% VA contacts averaged across the 2D contact fraction histograms), while the random copolymer has only ∼32% VA contacts. In the case of 75 mol % VA, even the random

https://dx.doi.org/10.1021/acsami.0c10747
ACS Appl. Mater. Interfaces 2020, 12, 47879−47890

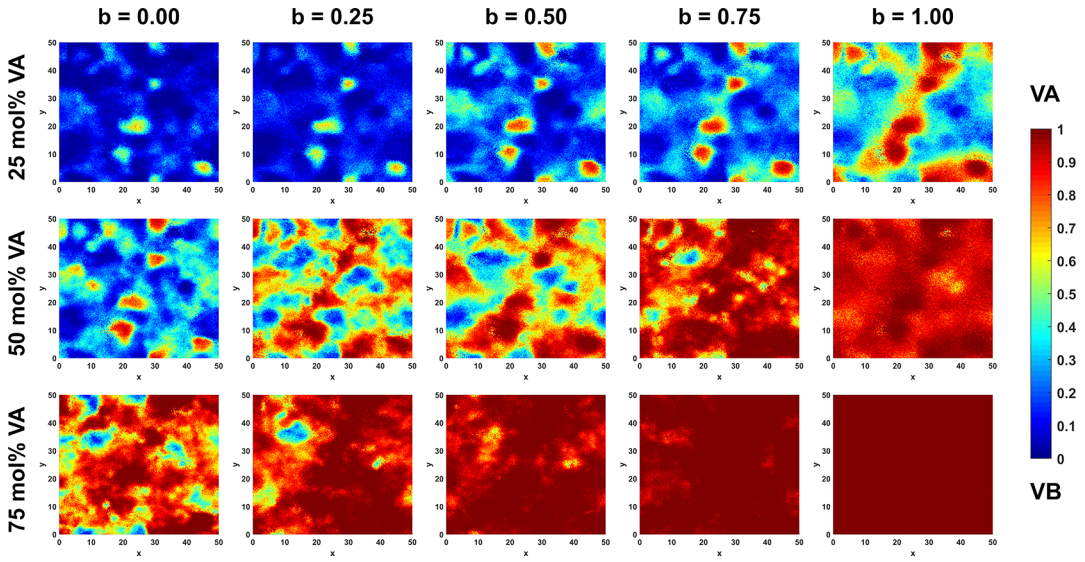

Figure 7. Contact fraction of VA monomers on the force-mapped silica surface as a function of *x*, *y*, VA content, and blockiness, histogramed over a 100 ns sampling period at 400 K. The 2D color maps correspond to the same selected trials as the 3D morphologies in Figure 6. We considered a monomer as contacting if it contains a bead whose lowest point lies within a 1 Å cutoff distance from a surface map.

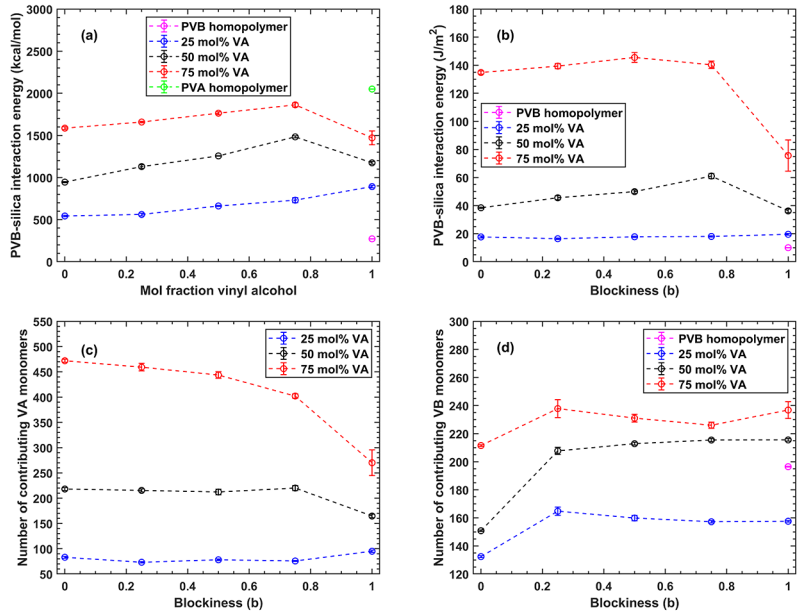

Figure 8. Adhesion energy in (a) kcal per mol of beads and (b) J/m^2, for the PVB−silica interface as a function of blockiness for varying amounts of VA and the numbers of (c) VA and (d) VB monomers contributing to the PVB−silica interaction energy. The numbers of contributing beads were defined by an energy cutoff of 1×10^{-3} cal/mol. The value of adhesion energy for the PVA homopolymer (417.9 ± 0.3 J/m^2) is omitted from the J/m^2 plot for clarity of the copolymer data. Likewise, excluded from the plot (c) is the number of interacting VA monomers for the PVA homopolymer (1089 ± 1). In all cases, averages are computed over the last 10 ns of the 150 ns simulation period at 400 K, and error bars represent the standard error of the mean of the three independent trials.

copolymer (b = 0.00) exhibits strong enrichment of VA at the silica interface (~80% VA contact fraction). At b = 0.25, the contact fraction is comparable to that of the 50 mol % VA diblock.

From the 2D contact fractions in Figure 7, the surface heterogeneity and the preference of VA monomers and VB monomers for different regions of the amorphous silica model are apparent. In each of the three independent trials for each overall VA content and blockiness, very similar behavior was observed. Shown here are the contact maps for one of the trials in each case. The patches and bands of dark red for 50 mol % VA at low blockiness and 25 mol % VA at moderate and high blockiness correspond to regions with a high density of surface hydroxyls in the all-atom model. The dark blue zones manifest regions with the lowest hydrophilicity in the contact maps for 75 mol % VA at low blockiness and 50 mol % VA at moderate blockiness.

Keeping in mind both the morphology away from the surface and the contact fraction maps, we now move on to the interaction energy between the PVB copolymer melts and silica, quantifying the adhesion strength. Figure 8 shows this total interaction energy in terms of energy per mol of beads,

https://dx.doi.org/10.1021/acsami.0c10747
ACS Appl. Mater. Interfaces 2020, 12, 47879−47890

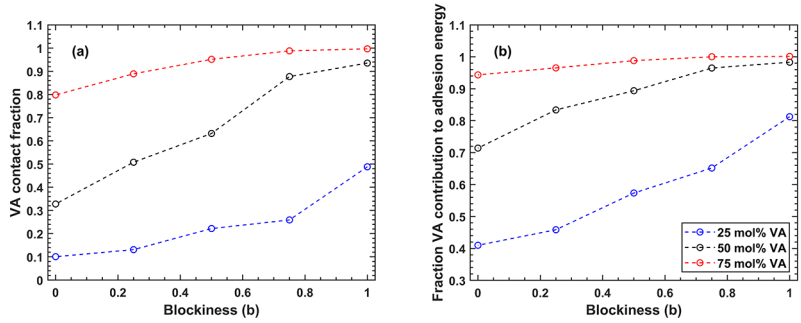

Figure 9. (a) Scalar contact fractions corresponding to the 2D contact area plots in Figure 7, averaged over all three independent trials. (b) Fractional contribution from the VA beads to overall adhesion energy, using an energy per mol of beads basis.

interaction energy per contact area, and numbers of contributing VA and VB beads, as a function of blockiness and VA content. We approximated the contact area of the rough surface as the solvent-accessible surface area,[64] computed in visual molecular dynamics (VMD)[65] using a probe radius of 1.75 Å, approximately the radius of the smallest of the SAFT-γ Mie PVB beads. Adhesion simulations of PVA and PVB homopolymers were also run for comparison, which, as expected, provide the strongest and weakest overall interaction energies, respectively. One should note that the PVB homopolymer interaction energy is likely underestimated here, as the PVB fused-sphere SAFT-γ Mie model underestimates the density of the PVB bulk homopolymer and, thus, the number of PVB beads interacting with the surface. The coarse-grained PVB model was optimized to accurately reproduce copolymer densities over the range of copolymer compositions studied here at the expense of PVB homopolymer properties, which are of little interest in the laminated safety glass interlayer application. Importantly, however, the density of diblock PVB copolymers was found to be correctly predicted. One should also realize that this PVB–silica interaction energy is merely an approximation for the true work of adhesion, in that it neglects the entropic contribution to the free energy of adhesion. As an alternative to the definition of interaction energy per unit area, work of adhesion can more rigorously be calculated from the surface tension of the "free" polymer, surface free energy of the solid substrate, and polymer–solid interfacial tension.[66,67] As we are interested in exploring the trends of adhesion strength with copolymer blockiness and VA content and quantitative comparison with commercial PVB resin data cannot be made with our simplified coarse-grained model, we chose not to perform more rigorous free energy calculations for each of the PVB copolymer melts. Despite the neglection of the entropic component and our use of a coarse-grained model that does not account for polarization effects or explicitly represent PVB stereochemistry, a remarkable agreement is obtained with the experimental work of adhesion results[45] for commercial PVB resins with different VA contents. The presence of additives in those samples precludes a more quantitative comparison with our results and thus a deduction of their blockiness.

At low VA content (25 mol %), adhesion energy in terms of kcal per mol of interacting beads increases monotonically with blockiness, and it is nearly insensitive to blockiness when converted to energy per unit area. From Figure 8, the numbers of contributing VA and VB beads mirror this. Interestingly, the effect of the increased coverage of VA with blockiness (Figure 7) on the adhesion energy is negated by changes in morphology away from the surface (Figure 6). At 50 and 75 mol % VA content, maxima in adhesion energy are observed not for diblocks, but for the case of moderately high blockiness. Similar results were reported by Jhon et al.[21] in a combined simulation and experimental study on the adsorption of poly(styrene-*co*-*p*-bromostyrene) (PSBrS) copolymers with varying degrees of blockiness onto silica. Random-blocky PSBrS copolymers exhibited higher adsorption from a good solvent onto silica than "truly random" copolymers with the same overall chemical composition, but diblocks did not provide maximum adsorption. Adsorption improved with blockiness but only until a temperature-dependent threshold was reached, at which an entropic penalty prevents total adsorption of the blocks which favor the surface.

Surprisingly, in terms of J/m^2, the PVB diblocks considered here exhibit the weakest interaction energy with the silica slab, despite the nearly complete coverage of the surface by the strongly interacting VA monomers. Morphology away from the substrate is largely responsible for this behavior. Upon an increase in blockiness from b = 0.75 to b = 1.00, there is a significant drop in the number of VA beads contributing to adhesion energy. In contrast, the number of contributing VB beads is roughly constant. Yet, the overall contributions from both VA monomers and VB monomers to adhesion energy fall sharply. While the decrease in contribution from the VA monomers is a clear consequence of increased phase segregation, the decrease in contribution from the VB monomers is a more subtle consequence of the much weaker interactions between the VB monomer and the silica slab and the decrease in local density in purely VB regions. Recall that the densities of PVA and PVB homopolymers are predicted to be approximately 1.19 and 0.92 g/cm^3, respectively, by our fused-sphere SAFT-γ Mie model.[47] Higher molecular weight PVB diblocks would be expected to exhibit stronger adhesion energy. Still, it remains to be seen if these would approach the PVA homopolymer limit and surpass the adhesion energy of the highly blocky copolymers considered here.

Variation in hydroxyl site density also contributes to the unexpectedly weak adhesion of the 50 mol % VA and 75 mol % VA diblocks. Regions of low hydroxyl density, where VB monomers contribute appreciably to adhesion, are populated almost entirely by VA monomers, while the VB monomers displaced farther from the surface contribute almost negligibly to the adhesion energy. Moderately blocky chains have the advantage that both VA and VB beads can migrate to their optimal adsorption zones. This phenomenon bears clear similarities to the concept of pattern recognition.[68] Future work will involve correlating the blockiness associated with the

https://dx.doi.org/10.1021/acsami.0c10747
ACS Appl. Mater. Interfaces 2020, 12, 47879–47890

hydroxyl sites with the adsorbing sequences of random-blocky copolymers.

Figure 9 plots the overall contact fraction scalar values calculated from the 2D contact maps (Figure 7) and the contribution of the VA monomers to the adhesion energies (Figure 8). The contact fraction and contribution from VA beads mirror each other, indicating that the contacting layer of beads is dominant in determining the overall adhesion energy. The VA beads are nearly entirely responsible for the PVB−silica interaction energy at b = 0.75 and 75 mol % VA, which exhibits the highest adhesion energy of any of the copolymers studied. The weak attraction of VB beads to certain surface regions is negated by repulsive interactions of VB beads located in other regions.

The classic tail−loop−train model[69] is useful in describing the statistics of the conformations of adsorbed polymers. In this model, *trains* represent contiguous stretches of adsorbed monomers, *loops* are stretches of nonadsorbed monomers between two trains, and *tails* are the portions of the chains that dangle away from the substrate and contain chain ends (Figure 2). From a thermodynamic perspective, trains represent the primary enthalpic driving force for polymer adhesion. For trains, the interaction energy between the polymer and the substrate must be strong enough to outweigh the severe penalty to configurational entropy that arises upon train formation. Loops and tails, in contrast, are much less restricted in the conformations available to them, and so they provide the entropic driving force for adhesion. Intuitively, monomers that possess strong attraction to the surface will promote the formation of trains, and monomers which have weak or unfavorable interactions with the surface will promote the occurrence of loops. Also contained in the loops are monomers which favor the surface but are unable to adsorb due to conformational restrictions. Figure 10 shows the average

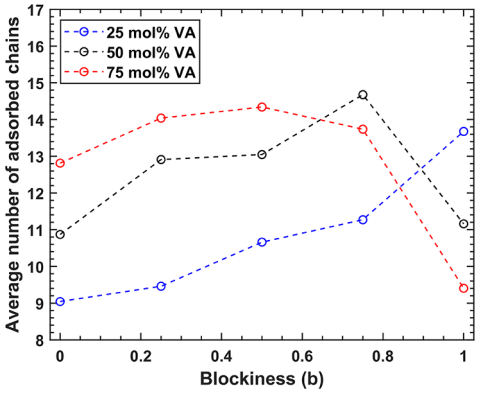

Figure 10. Average number of chains containing at least one adsorbed monomer as a function of blockiness for the given VA monomer contents. Averages are taken over the last 100 ns at 400 K, and over three independent trials.

number of chains with at least one adsorbed monomer, and Figure 11 shows the average numbers of VA and VB monomers in loops, trains, and tails per adsorbed chain, as functions of VA content and blockiness parameter. Compositions of the trains, loops, and tails in terms of volume fraction of VA monomers are shown in Figure 12. The average numbers of trains, loops, and tails per adsorbed chain are also plotted in the Supporting Information (Figure S36). Surprisingly, for a given VA content, the length distributions of trains were found to be affected very little by blockiness (Figure S35). Loop length distributions were similarly unaffected by blockiness, except for the 50 mol % VA and 75 mol % VA diblocks, which exhibited a strong preference for short loops. As evident from Figure 12, these short loops are made up nearly exclusively of VA monomers, while the VB monomers are concentrated in tails. In general, for a given VA content, the VA volume fraction in trains and loops increases with blockiness, and the VA volume fraction in tails decreases with blockiness, consistent with the morphologies shown in Figure 6. The numbers of VA and VB monomers in loops per adsorbed chain also reflect the morphology in the vicinity of the surface. For all VA fractions, the average number of VA monomers in trains per adsorbed chain increases with blockiness, while the number of VB monomers in trains decreases with increasing blockiness. This is consistent with the VA contact fractions shown in Figure 9.

For 25 mol % VA, the number of adsorbed chains increases monotonically with increasing blockiness, which can again be explained by the 3D morphology in Figure 6. The small blocks of VA monomers in each chain near the surface can migrate to the surface with relatively little competition from other VA monomers for the high hydroxyl density regions on the surface. A similar surface enrichment of the comonomer type with stronger attraction to the surface was observed in an experimental study which characterized poly(ethylene-*stat*-vinyl acetate) (PEVAc) adsorption to fumed silica.[70] With increasing blockiness, fewer VB monomers interfere with the adsorption of the VA blocks. For 50 mol % VA and 75 mol % VA, the number of adsorbed chains drops sharply upon increasing the blockiness from b = 0.75 to b = 1.00, likely a consequence of increased competition for the high hydroxyl density regions. In spite of this, the overall number of VA monomers involved in trains per adsorbed chain increases. Given that the train length distributions are not appreciably affected by blockiness, this means that more trains are present. The short lengths of these trains could be related to the hydroxyl site spatial distribution on the surface—the presence of relatively hydrophobic patches likely leads to short VA loops discussed in the preceding paragraph, with small voids in these hydrophobic regions in the case of the 75 mol % VA diblock.

While we have systematically varied the overall blockiness with the aim of understanding trends in interfacial behavior, further optimization of PVB adhesion strength could be performed by varying individual VA and VB monomer positions in the sequences. In a study by Zheligovskaya et al.,[20] an inverse design strategy was used to create adsorption-tuned A/B copolymers. The resulting optimal sequences were so-called "protein-like copolymers" characterized by highly disperse, non-Poisson distributions in block lengths and exhibited a higher concentration of the monomer type which interacts more strongly with the surface in the middle of the chain sequences than at the ends. Similar conclusions as to the importance of high block polydispersity in adsorption behavior were made by Jhon et al. from Monte Carlo simulations[21] of single-chain adsorption of blocky poly(styrene-*co*-*p*-bromostyrene) copolymers from solution and by Meenakshisundaram et al.[12] from optimal A/B compatibilizer sequences found using a genetic algorithm and MD simulations. Such optimal sequences for the PVB system could, in principle, be discovered using inverse design and/or machine-learning approaches. This would, however, require a herculean computational effort because of the simulation time needed to equilibrate the interfacial PVB systems, and the

https://dx.doi.org/10.1021/acsami.0c10747
ACS Appl. Mater. Interfaces 2020, 12, 47879−47890

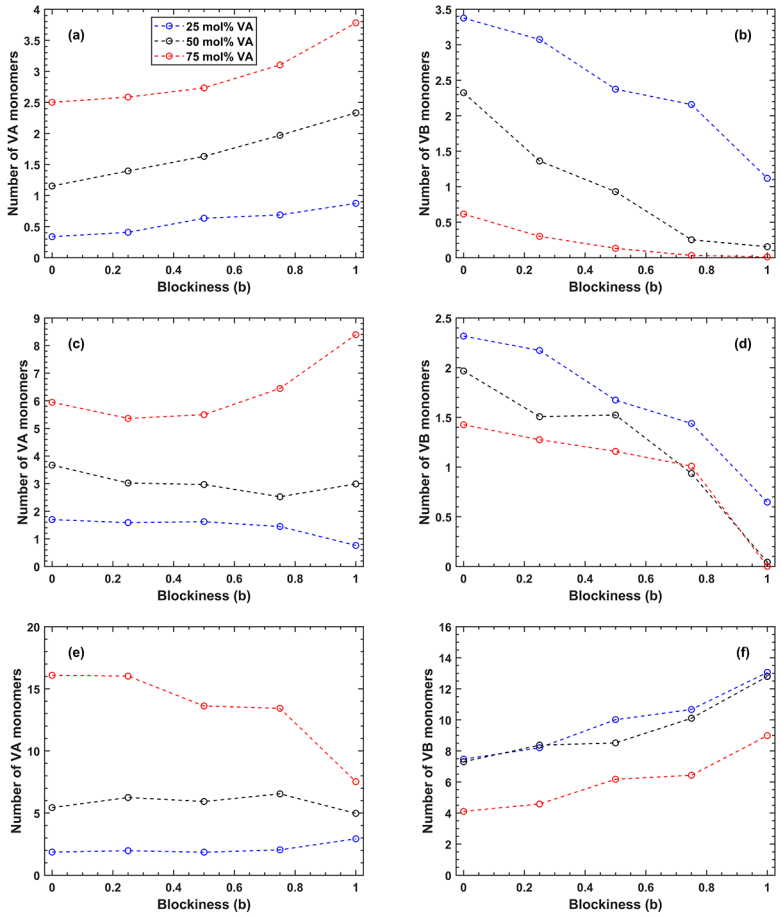

Figure 11. Average numbers of VA monomers in (a) trains, (c) loops, and (e) tails and VB monomers in (b) trains, (d) loops, and (f) tails per adsorbed chain (i.e., normalized by the data in Figure 10), as a function of blockiness for given VA monomer contents. Averages are taken over the last 100 ns at 400 K and over the three independent trials.

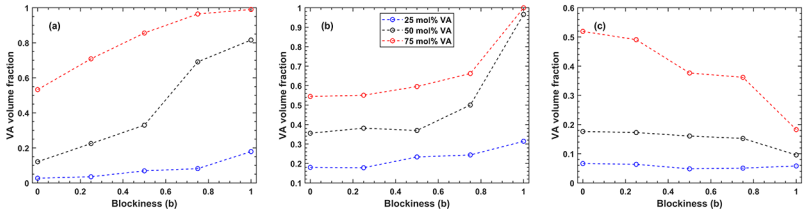

Figure 12. Average overall volume fraction of VA monomers within all (a) trains, (b) loops, and (c) tails as a function of blockiness for the given VA monomer contents. Averages are taken over the last 100 ns at 400 K and over three independent trials. Monomer volumes are defined by their Mie radii, as described earlier.

solution would likely be dependent on the precise distribution of hydroxyl groups on the amorphous silica model.

4. CONCLUSIONS

We performed coarse-grained molecular dynamics simulations of PVB copolymers at a force-mapped realistic hydroxylated amorphous silica surface for a series of VA contents and comonomer blockiness. While PVB adhesion energy to silica increased with increasing VA content as expected, a complex dependence of adhesion energy and interfacial structure on the blockiness parameter was discovered, particularly, for the cases of comparable volume fractions of VA and VB monomers. For 50 and 75 mol % VA monomers, PVB copolymers with moderately high blockiness (b = 0.50−0.75) exhibited higher adhesion strength than the corresponding diblocks. We attributed this to the following underlying causes: (1) the nontrivial contribution of VB monomers to adhesion energy, (2) variation in hydroxyl site density on the amorphous silica surface, and (3) the disparity in self-interaction strengths of the VA and VB monomers which drives phase segregation.

The use of a chemically heterogeneous surface allows for both VA and VB monomers in non-diblock copolymers to adsorb to their preferred sites and provide maximal contributions to adhesion energy. In the diblocks with a high VA content, the formation of VA lamellae at the interface with silica not only eliminates the contribution of VB monomers to adhesion energy but also reduces the total number of VA monomers interacting with the surface as well. Nonobvious trends in the numbers of adsorbed chains and loop/train/tail statistics as a function of blockiness indicate that what is understood about polymer

https://dx.doi.org/10.1021/acsami.0c10747
ACS Appl. Mater. Interfaces 2020, 12, 47879−47890

adsorption in terms of simple uniform surface models may no longer apply for chemically heterogeneous substrates. Repetition of this study on random-blocky PVB adsorption with a crystalline silica surface, such as quartz or cristobalite, would clarify which of the behaviors observed here originates from the surface heterogeneity and which of the behaviors stems from the polymer−polymer and polymer−surface interactions. This will be a topic of future work.

Future studies on the effects of the finite size of the simulation cell and the effect of molecular weights of the PVB chains would also be informative. The feature sizes of the morphologies shown in Figure 6 would change with box size and the amount of PVB chains in the simulation cell. Ideally, enough chains and a large enough silica slab model should be used such that morphology away from the surface converges to that of bulk PVB. It would be interesting to test if high-molecular weight PVB chains exhibit similar trends in adhesion energy as a function of blockiness, and whether high-molecular weight diblock PVB chains approach the performance of the PVA homopolymer.

Experimental impact testing and work of adhesion measurements would need to be carried out for a series of PVB/glass samples with varying blockiness and vinyl alcohol contents to further validate the simulation results of this study and to truly optimize the fracture toughness of glass/PVB/glass composite materials. At present, there are two major impediments to carrying out these experiments: (1) the inability to synthesize PVB copolymers with controllable block length distributions and (2) the lack of a characterization technique that can reliably identify the sequence distributions of PVB copolymers.

Copolymer blockiness is a key parameter for tuning adhesion properties and interfacial structure and can have as much as an effect as changing the chemical composition. As a deeper understanding of structure−property relationships for random-blocky and other sequence-controlled polymers is developed and synthetic techniques for controlling copolymer sequences progress further, the performance of copolymer materials can be improved by tailoring their monomer sequences.

■ ASSOCIATED CONTENT

Supporting Information

The Supporting Information is available free of charge at https://pubs.acs.org/doi/10.1021/acsami.0c10747.

> Detailed description of force-mapping procedure; PVB−silica contact maps for each of the PVB coarse-grained bead types; contact fraction 2D histograms for all three independent trials of each blockiness and VA content, PVB−silica interfacial morphology renderings for all three independent trials of each blockiness and VA content; 1D volume fraction profiles of VA monomers as a function of distance from the silica surface; and supplemental adhesion and loop, train, and tail statistics (PDF)

■ AUTHOR INFORMATION

Corresponding Author

Erik E. Santiso − *Department of Chemical and Biomolecular Engineering, North Carolina State University, Raleigh, North Carolina 27695, United States;* orcid.org/0000-0003-1768-8414; Email: eesantis@ncsu.edu

Authors

Christopher C. Walker − *Department of Chemical and Biomolecular Engineering, North Carolina State University, Raleigh, North Carolina 27695, United States*

Jan Genzer − *Department of Chemical and Biomolecular Engineering, North Carolina State University, Raleigh, North Carolina 27695, United States;* orcid.org/0000-0002-1633-238X

Complete contact information is available at: https://pubs.acs.org/10.1021/acsami.0c10747

Author Contributions

The manuscript was written through the contributions of all authors. All authors have given approval to the final version of the manuscript.

Notes

The authors declare no competing financial interest.

■ ACKNOWLEDGMENTS

We acknowledge Dr. Iacovella and the Cummings and McCabe groups in the Department of Chemical Engineering at Vanderbilt University for kindly providing the amorphous silica topology files. We acknowledge the Eastman Chemical Company for providing financial support and guidance for this project, as well as financial support from NSF award #1704151.

■ REFERENCES

(1) Hallensleben, M. L.; Fuss, R.; Mummy, F. Polyvinyl Compounds, Others. In *Ullmann's Encyclopedia of Industrial Chemistry*; Wiley-VCH: Weinheim, 2015.

(2) Kennar, G. A. Interlayer for Laminated Safety Glass. U.S. Patent 4,035,549 A, 1977.

(3) Sha, Y.; Hui, C. Y.; Kramer, E. J.; Garrett, P. D.; Knapczyk, J. W. Analysis of Adhesion and Interface Debonding in Laminated Safety Glass. *J. Adhes. Sci. Technol.* **1997**, *11*, 49−63.

(4) Bennison, S. J.; Jagota, A.; Smith, C. A. Fracture of Glass/Poly(vinyl butyral) (Butacite) Laminates in Biaxial Flexure. *J. Am. Ceram. Soc.* **1999**, *82*, 1761−1770.

(5) Chen, W.; Karagiannis, A. High Impact Polymer Interlayers. U.S. Patent 9,248,599 B2, 2016.

(6) Teotia, M.; Soni, R. K. Polymer Interlayers for Glass Lamination - A Review. *Int. J. Sci. Res.* **2012**, *3*, 1264−1270.

(7) Olabisi, O.; Adewale, K. *Handbook of Thermoplastics*, 2nd ed.; Taylor & Francis Group: Boca Raton, Fl, 2016.

(8) Martens, S.; Holloway, J. O.; Du Prez, F. E. Click and Click-Inspired Chemistry for the Design of Sequence-Controlled Polymers. *Macromol. Rapid Commun.* **2017**, *38*, 1700469.

(9) Szymański, J. K.; Abul-Haija, Y. M.; Cronin, L. Exploring Strategies to Bias Sequence in Natural and Synthetic Oligomers and Polymers. *Acc. Chem. Res.* **2018**, *51*, 649−658.

(10) Lutz, J.-F.; Ouchi, M.; Liu, D. R.; Sawamoto, M. Sequence-Controlled Polymers. *Science* **2013**, *341*, 1238149.

(11) *Sequence-Controlled Polymers*; Lutz, J.-F., Ed.; Wiley-VCH: Weinheim, 2018.

(12) Meenakshisundaram, V.; Hung, J.-H.; Patra, T. K.; Simmons, D. S. Designing Sequence-Specific Copolymer Compatibilizers Using a Molecular-Dynamics-Simulation-Based Genetic Algorithm. *Macromolecules* **2017**, *50*, 1155−1166.

(13) Lytle, T. K.; Chang, L.-W.; Markiewicz, N.; Perry, S. L.; Sing, C. E. Designing Electrostatic Interactions via Polyelectrolyte Monomer Sequence. *ACS Cent. Sci.* **2019**, *5*, 709−718.

(14) Khadilkar, M. R.; Paradiso, S.; Delaney, K. T.; Fredrickson, G. H. Inverse Design of Bulk Morphologies in Multiblock Polymers Using Particle Swarm Optimization. *Macromolecules* **2017**, *50*, 6702−6709.

(15) Fierens, S. K.; Telitel, S.; Van Steenberge, P. H. M.; Reyniers, M.-F.; Marin, G. B.; Lutz, J.-F.; D'hooge, D. R. Model-Based Design To

Push the Boundaries of Sequence Control. *Macromolecules* **2016**, *49*, 9336−9344.
(16) D'hooge, D. R.; Van Steenberge, P. H. M.; Derboven, P.; Reyniers, M.-F.; Marin, G. B. Model-Based Design of the Polymer Microstructure: Bridging the Gap between Polymer Chemistry and Engineering. *Polym. Chem.* **2015**, *6*, 7081−7096.
(17) Rosales, A. M.; Segalman, R. A.; Zuckermann, R. N. Polypeptoids: A Model System to Study the Effect of Monomer Sequence on Polymer Properties and Self-Assembly. *Soft Matter* **2013**, *9*, 8400−8414.
(18) Genzer, J.; Khalatur, P. G.; Khokhlov, A. R. *6.18—Conformation-Dependent Design of Synthetic Functional Copolymers*; Elsevier B.V., 2012; Vol. *6*.
(19) Khokhlov, A. R.; Khalatur, P. G. Protein-like Copolymers: Computer Simulation. *Phys. Stat. Mech. Appl.* **1998**, *249*, 253−261.
(20) Zheligovskaya, E. A.; Khalatur, P. G.; Khokhlov, A. R. Properties ofABcopolymers with a special adsorption-tuned primary structure. *Phys. Rev. E: Stat. Phys., Plasmas, Fluids, Relat. Interdiscip. Top.* **1999**, *59*, 3071−3078.
(21) Jhon, Y. K.; Semler, J. J.; Genzer, J.; Beevers, M.; Gus'kova, O. A.; Khalatur, P. G.; Khokhlov, A. R. Effect of Comonomer Sequence Distribution on the Adsorption of Random Copolymers onto Impenetrable Flat Surfaces. *Macromolecules* **2009**, *42*, 2843−2853.
(22) Khaira, G. S.; Qin, J.; Garner, G. P.; Xiong, S.; Wan, L.; Ruiz, R.; Jaeger, H. M.; Nealey, P. F.; De Pablo, J. J. Evolutionary Optimization of Directed Self-Assembly of Triblock Copolymers on Chemically Patterned Substrates. *ACS Macro Lett.* **2014**, *3*, 747−752.
(23) Qin, J.; Khaira, G. S.; Su, Y.; Garner, G. P.; Miskin, M.; Jaeger, H. M.; De Pablo, J. J. Evolutionary Pattern Design for Copolymer Directed Self-Assembly. *Soft Matter* **2013**, *9*, 11467−11472.
(24) Paradiso, S. P.; Delaney, K. T.; Fredrickson, G. H. Swarm Intelligence Platform for Multiblock Polymer Inverse Formulation Design. *ACS Macro Lett.* **2016**, *5*, 972−976.
(25) Potestio, R.; Peter, C.; Kremer, K. Computer Simulations of Soft Matter: Linking the Scales. *Entropy* **2014**, *16*, 4199−4245.
(26) Brini, E.; Algaer, E. A.; Ganguly, P.; Li, C.; Rodríguez-Ropero, F.; van der Vegt, N. F. A. Systematic coarse-graining methods for soft matter simulations - a review. *Soft Matter* **2013**, *9*, 2108.
(27) Müller-Plathe, F. Coarse-Graining in Polymer Simulation: From the Atomistic to the Mesoscopic Scale and Back. *ChemPhysChem* **2002**, *3*, 754−769.
(28) Gooneie, A.; Schuschnigg, S.; Holzer, C. A Review of Multiscale Computational Methods in Polymeric Materials. *Polymers* **2017**, *9*, 16.
(29) Arora, A.; Qin, J.; Morse, D. C.; Delaney, K. T.; Fredrickson, G. H.; Bates, F. S.; Dorfman, K. D. Broadly Accessible Self-Consistent Field Theory for Block Polymer Materials Discovery. *Macromolecules* **2016**, *49*, 4675−4690.
(30) Ganesan, V.; Kumar, N. A.; Pryamitsyn, V. Blockiness and Sequence Polydispersity Effects on the Phase Behavior and Interfacial Properties of Gradient Copolymers. *Macromolecules* **2012**, *45*, 6281−6297.
(31) Jiang, R.; Wang, Z.; Yin, Y.; Li, B.; Shi, A.-C. Effects of Compositional Polydispersity on Gradient Copolymer Melts. *J. Chem. Phys.* **2013**, *138*, 074906.
(32) Theodorou, D. N.; Vogiatzis, G. G.; Kritikos, G. Self-Consistent-Field Study of Adsorption and Desorption Kinetics of Polyethylene Melts on Graphite and Comparison with Atomistic Simulations. *Macromolecules* **2014**, *47*, 6964−6981.
(33) Schweizer, K. S.; Curro, J. G. PRISM Theory of the Structure, Thermodynamics, and Phase Transitions of Polymer Liquids and Alloys. In *Atomistic Modeling of Physical Properties*; Monnerie, L., Suter, U. W., Eds.; Advances in Polymer Science; Springer: Berlin, Heidelberg, 1994; Vol. *116*, pp 319−377.
(34) Martin, T. B.; Gartner, T. E.; Jones, R. L.; Snyder, C. R.; Jayaraman, A. PyPRISM: A Computational Tool for Liquid-State Theory Calculations of Macromolecular Materials. *Macromolecules* **2018**, *51*, 2906−2922.
(35) Mortazavian, H.; Fennell, C. J.; Blum, F. D. Structure of the Interfacial Region in Adsorbed Poly(Vinyl Acetate) on Silica. *Macromolecules* **2016**, *49*, 298−307.
(36) Mortazavian, H.; Fennell, C. J.; Blum, F. D. Surface Bonding Is Stronger for Poly(Methyl Methacrylate) than for Poly(Vinyl Acetate). *Macromolecules* **2016**, *49*, 4211−4219.
(37) Linse, P.; Källrot, N. Polymer Adsorption from Bulk Solution onto Planar Surfaces: Effect of Polymer Flexibility and Surface Attraction in Good Solvent. *Macromolecules* **2010**, *43*, 2054−2068.
(38) Mao, C. M.; Sampath, J.; Sprenger, K. G.; Drobny, G.; Pfaendtner, J. Molecular Driving Forces in Peptide Adsorption to Metal Oxide Surfaces. *Langmuir* **2019**, *35*, 5911−5920.
(39) Baschnagel, J.; Meyer, H.; Varnik, F.; Metzger, S.; Aichele, M.; Müller, M.; Binder, K. Computer Simulations of Polymers Close to Solid Interfaces: Some Selected Topics. *Interface Sci.* **2003**, *11*, 159−173.
(40) Welch, D.; Lettinga, M. P.; Ripoll, M.; Dogic, Z.; Vliegenthart, G. A. Trains, Tails and Loops of Partially Adsorbed Semi-Flexible Filaments. *Soft Matter* **2015**, *11*, 7507−7514.
(41) Johnston, K.; Harmandaris, V. Hierarchical Simulations of Hybrid Polymer-Solid Materials. *Soft Matter* **2013**, *9*, 6696−6710.
(42) Kłos, J. S.; Romeis, D.; Sommer, J.-U. Adsorption of Random Copolymers from a Melt onto a Solid Surface: Monte Carlo Studies. *J. Chem. Phys.* **2010**, *132*, 024907.
(43) Yang, Q.-H.; Luo, M.-B. Dynamics of Adsorbed Polymers on Attractive Homogeneous Surfaces. *Sci. Rep.* **2016**, *6*, 37156.
(44) Tatek, Y. B.; Tsige, M. Structural Properties of Atactic Polystyrene Adsorbed onto Solid Surfaces. *J. Chem. Phys.* **2011**, *135*, 174708.
(45) Nguyen, F. N.; Berg, J. C. The Effect of Vinyl Alcohol Content on Adhesion Performance in Poly(Vinyl Butyral)/Glass Systems. *J. Adhes. Sci. Technol.* **2004**, *18*, 1011−1026.
(46) Papaioannou, V.; Lafitte, T.; Avendaño, C.; Adjiman, C. S.; Jackson, G.; Müller, E. A.; Galindo, A. Group Contribution Methodology Based on the Statistical Associating Fluid Theory for Heteronuclear Molecules Formed from Mie Segments. *J. Chem. Phys.* **2014**, *140*, 054107.
(47) Walker, C. C.; Genzer, J.; Santiso, E. E. Extending the fused-sphere SAFT-γ Mie force field parameterization approach to poly(vinyl butyral) copolymers. *J. Chem. Phys.* **2020**, *152*, 044903.
(48) Walker, C. C.; Genzer, J.; Santiso, E. E. Development of a fused-sphere SAFT-γ Mie force field for poly(vinyl alcohol) and poly-(ethylene). *J. Chem. Phys.* **2019**, *150*, 034901.
(49) Herdes, C.; Ervik, Å.; Mejía, A.; Müller, E. A. Prediction of the water/oil interfacial tension from molecular simulations using the coarse-grained SAFT-γ Mie force field. *Fluid Phase Equilib.* **2018**, *476*, 9−15.
(50) Theodorakis, P. E.; Müller, E. A.; Craster, R. V.; Matar, O. K. Superspreading: Mechanisms and Molecular Design. *Langmuir* **2015**, *31*, 2304−2309.
(51) Herdes, C.; Santiso, E. E.; James, C.; Eastoe, J.; Müller, E. A. Modelling the Interfacial Behaviour of Dilute Light-Switching Surfactant Solutions. *J. Colloid Interface Sci.* **2015**, *445*, 16−23.
(52) Rahman, S.; Lobanova, O.; Jiménez-Serratos, G.; Braga, C.; Raptis, V.; Müller, E. A.; Jackson, G.; Avendaño, C.; Galindo, A. SAFT-γ Force Field for the Simulation of Molecular Fluids. 5. Hetero-Group Coarse-Grained Models of Linear Alkanes and the Importance of Intramolecular Interactions. *J. Phys. Chem. B* **2018**, *122*, 9161−9177.
(53) Morgado, P.; Lobanova, O.; Müller, E. A.; Jackson, G.; Almeida, M.; Filipe, E. J. M. SAFT-γ force field for the simulation of molecular fluids: 8. Hetero-segmented coarse-grained models of perfluoroalky-lalkanes assessed with new vapour-liquid interfacial tension data. *Mol. Phys.* **2016**, *114*, 2597−2614.
(54) Ghobadi, A. F.; Elliott, J. R. Adapting SAFT-γ perturbation theory to site-based molecular dynamics simulation. II. Confined fluids and vapor-liquid interfaces. *J. Chem. Phys.* **2014**, *141*, 024708.
(55) Xi, S.; Wang, L.; Liu, J.; Chapman, W. Thermodynamics, Microstructures, and Solubilization of Block Copolymer Micelles by Density Functional Theory. *Langmuir* **2019**, *35*, 5081−5092.

https://dx.doi.org/10.1021/acsami.0c10747
ACS Appl. Mater. Interfaces 2020, 12, 47879−47890

(56) Dominik, A.; Tripathi, S.; Chapman, W. G. Bulk and Interfacial Properties of Polymers from Interfacial SAFT Density Functional Theory. *Ind. Eng. Chem. Res.* **2006**, *45*, 6785−6792.
(57) Black, J. E.; Iacovella, C. R.; Cummings, P. T.; McCabe, C. Molecular Dynamics Study of Alkylsilane Monolayers on Realistic Amorphous Silica Surfaces. *Langmuir* **2015**, *31*, 3086−3093.
(58) Van Duin, A. C. T.; Dasgupta, S.; Lorant, F.; Goddard, W. A. ReaxFF: A Reactive Force Field for Hydrocarbons. *J. Phys. Chem. A* **2001**, *105*, 9396−9409.
(59) Zhuravlev, L. T. The Surface Chemistry of Amorphous Silica. Zhuravlev Model. *Colloids Surf., A* **2000**, *173*, 1−38.
(60) Jorgensen, W. L.; Maxwell, D. S.; Tirado-Rives, J. Development and Testing of the OPLS All-Atom Force Field on Conformational Energetics and Properties of Organic Liquids. *J. Am. Chem. Soc.* **1996**, *118*, 11225−11236.
(61) Lorenz, C. D.; Webb, E. B.; Stevens, M. J.; Chandross, M.; Grest, G. S. Frictional Dynamics of Perfluorinated Self-Assembled Monolayers on Amorphous SiO2. *Tribol. Lett.* **2005**, *19*, 93−98.
(62) Plimpton, S. Fast Parallel Algorithms for Short-Range Molecular Dynamics. *J. Comput. Phys.* **1995**, *117*, 1−19.
(63) Martínez, L.; Andrade, R.; Birgin, E. G.; Martínez, J. M. Packmol: A Package for Building Initial Configurations for Molecular Dynamics Simulations. *J. Comput. Chem.* **2009**, *30*, 2157−2164.
(64) Lee, B.; Richards, F. M. The Interpretation of Protein Structures: Estimation of Static Accessibility. *J. Mol. Biol.* **1971**, *55*, 379−IN4.
(65) Humphrey, W.; Dalke, A.; Schulten, K. VMD: Visual Molecular Dynamics. *J. Mol. Graph.* **1996**, *14*, 33−38.
(66) Sgouros, A. P.; Vogiatzis, G. G.; Kritikos, G.; Boziki, A.; Nikolakopoulou, A.; Liveris, D.; Theodorou, D. N. Molecular Simulations of Free and Graphite Capped Polyethylene Films: Estimation of the Interfacial Free Energies. *Macromolecules* **2017**, *50*, 8827−8844.
(67) Sgouros, A. P.; Vogiatzis, G. G.; Megariotis, G.; Tzoumanekas, C.; Theodorou, D. N. Multiscale Simulations of Graphite-Capped Polyethylene Melts: Brownian Dynamics/Kinetic Monte Carlo Compared to Atomistic Calculations and Experiment. *Macromolecules* **2019**, *52*, 7503−7523.
(68) Jayaraman, A.; Hall, C. K.; Genzer, J. Designing Pattern-Recognition Surfaces for Selective Adsorption of Copolymer Sequences Using Lattice Monte Carlo Simulation. *Phys. Rev. Lett.* **2005**, *94*, 078103.
(69) Jones, R. A. L.; Richard, R. W. *Polymers at Surfaces and Interfaces*; Cambridge University Press: Cambridge, 1999.
(70) Maddumaarachchi, M.; Blum, F. D. Thermal Analysis and FT-IR Studies of Adsorbed Poly(Ethylene-Stat-Vinyl Acetate) on Silica. *J. Polym. Sci., Part B: Polym. Phys.* **2014**, *52*, 727−736.

https://dx.doi.org/10.1021/acsami.0c10747
ACS Appl. Mater. Interfaces 2020, 12, 47879−47890